Bioactive Materials 2 (2017) 146–155

Contents lists available at ScienceDirect

Bioactive Materials

journal homepage: http://www.keaipublishing.com/en/journals/bioactive-materials/

In-situ solvothermal processing of polycaprolactone/hydroxyapatite nanocomposites with enhanced mechanical and biological performance for bone tissue engineering

Saeed Moeini [a], Mohammad Reza Mohammadi [a], Abdolreza Simchi [a, b, *]

[a] Department of Materials Science and Engineering, Sharif University of Technology, Tehran, Iran
[b] Institute for Nanoscience and Nanotechnology, Sharif University of Technology, Tehran, Iran

ARTICLE INFO

Article history:
Received 22 February 2017
Accepted 13 April 2017
Available online 21 April 2017

Keywords:
Nanocomposite
Polycaprolactone
Hydroxyapatite
Mechanical property
Cytotoxicity

ABSTRACT

The interest in biodegradable polymer-matrix nanocomposites with bone regeneration potential has been increasing in recent years. In the present work, a solvothermal process is introduced to prepare hydroxyapatite (HA) nanorod-reinforced polycaprolactone *in-situ*. A non-aqueous polymer solution containing calcium and phosphorous precursors is prepared and processed in a closed autoclave at different temperatures in the range of 60–150 °C. Hydroxyapatite nanorods with varying aspect ratios are formed depending on the processing temperature. X-ray diffraction analysis and field-emission scanning electron microscopy indicate that the HA nanorods are semi-crystalline. Energy-dispersive X-ray spectroscopy and Fourier transform infrared spectrometry determine that the ratio of calcium to phosphorous increases as the processing temperature increases. To evaluate the effect of *in-situ* processing on the mechanical properties of the nanocomposites, highly porous scaffolds (>90%) containing HA nanorods are prepared by employing freeze drying and salt leaching techniques. It is shown that the elastic modulus and strength of the nanocomposites prepared by the *in-situ* method is superior (~15%) to those of the *ex-situ* samples (blended HA nanorods with the polymer solution). The enhanced bone regeneration potential of the nanocomposites is shown via an *in vitro* bioactivity assay in a saturated simulated body fluid. An improved cell viability and proliferation is also shown by employing (3-(4,5-dimethylthiazol-2-yl)-2, 5-diphenyl tetrazolium bromide) (MTT) assay in human osteosarcoma cell lines. The prepared scaffolds with *in vitro* regeneration capacity could be potentially useful for orthopaedic applications and maxillofacial surgery.

1. Introduction

Tissue engineering offers a new approach to regenerate diseased or damaged tissues such as bone [1]. The rapidly growing research in the bone tissue engineering area provides a new and promising approach for bone repair and regeneration [2]. Bone is a natural organic–inorganic composite consisting of collagen fibrils containing embedded, well-arrayed, nanocrystalline and plate-like inorganic materials with length of 25–50 nm [3,4]. Hydroxyapatite (HA), which is chemically similar to the inorganic component of bone matrix, has been proved to be an osteoconductive material [5] with affinity toward many adhesive proteins and direct involvement in the bone cell differentiation and mineralization processes [6]. The close chemical similarity of HA to natural bone has led to extensive research efforts to use synthetic HA as a bone substitute and/or replacement in biomedical applications [7]. However, HA shows poor biomechanical properties such as high brittleness as well as low fatigue strength and flexibility that limit its load-bearing applications [8]. As a result, synthesis of HA particles with various sizes and morphologies and distribution of them inside biodegradable polymer matrixes have attracted significant interest in recent years [9]. The idea of combining bioactive ceramics and degradable polymers to produce three-dimensional (3D) scaffolds with high porosity is a promising strategy for the design and development of composite systems for bone tissue

* Corresponding author. Department of Materials Science and Engineering, Sharif University of Technology, Tehran, Iran.
E-mail address: simchi@sharif.edu (A. Simchi).
Peer review under responsibility of KeAi Communications Co., Ltd.

http://dx.doi.org/10.1016/j.bioactmat.2017.04.004

engineering [10]. Many composite scaffolds have been prepared either by distributing HA nanoparticles within a polymer matrix or by the mineralization of HA nanoparticles on the surface of polymeric substrates [10–13]. Much work has also been performed on the processing and applications of HA nanorods for bone tissue engineering as the bioactivity and mechanical properties are significantly enhanced compared to irregular-shaped particles [14–18].

In the present work, polycaprolactone (PCL) nanocomposites containing HA nanorods were prepared by *in-situ* solvothermal techniques. Polycaprolactone is a biodegradable polymer with remarkable toughness and good biocompatibility [19]. It is a semi-crystalline aliphatic polymer that has a slower degradation rate and higher fracture energy than most biocompatible polymers [20–23]. The intrinsic hydrophobic chemical nature of PCL as well as its poor surface wetting and interactions with biological fluids avoid cell adhesion and proliferation [11]. It has recently been shown that the biological and mechanical properties of PCL scaffolds can be tailored by osteogenic and osteoinductive inorganic phases, promoting bone regeneration [24–27]. Chen el al. [28] observed that relative cell survival of PCL-HA composites exceeded that of neat PCL and control samples in MTT assay. Nevertheless, poor interfacial adhesion is often observed when HA particles are *ex-situ* dispersed in a polymer matrix (due to different chemical nature of the components and their surface energy). Consequently, the *ex-situ* prepared composites may exhibit degraded mechanical properties. Li et al. [29] reported that surface treatment of HA nanoparticles by a kind of silane (ɣ-glycioxypropyltrimethoxysilane), aiming to improve mechanical properties of PCL-HA composite, led to relative aggravation in biocompatibility and bioactivity (although the resulted values still exceeded that of control sample). A promising strategy to improve the distribution of the bioceramic in the polymer matrix with higher degree of phase interaction between the polymer and the inorganic filler is to synthesize the HA nanoparticles *in-situ* during processing of the scaffolds [11,30]. This procedure would avoid the extensive particle agglomeration typically seen in composites obtained by mechanical incorporation of HA particles into the polymer melt or solution [11]. Recently, co-precipitation and sol-gel methods have been utilized to synthesize HA nanoparticles-reinforced PCL nanocomposites [30–32]. Owing to the superior properties of HA nanorods, a few attempts have also made on processing of poly (D, L-lactide) (PDLLA) and polyvinyl alcohol (PVA) composites by employing solvothermal processes [33,34]. While the former polymer is expensive, the latter has weak mechanical characteristics. Therefore, we have adopted a new strategy for *in-situ* preparation of HA nanorods in the PCL matrix with fine particle distribution. Polycaprolactone is a FDA approved polymer which is relatively cheap with reliable mechanical strength [10,11,21]. Highly porous scaffolds (>90%) were prepared by salt leaching/freeze-drying techniques and their physicochemical, biological and mechanical properties were examined. The potential and benefits of the *in-situ* solvothermal processing compared to the ex-situ method is shown.

2. Experimental

2.1. Materials

Calcium hydrate ($Ca(OH)_2$, Acros, USA) and phosphoric acid (85% H_3PO_4, Merck, Germany) were used as Ca and P precursors for the synthesis of PCL/HA nanocomposites. Polycaprolactone with an average molecular weight of 80,000 was supplied by Sigma-Aldrich (USA). Analytical grades of acetone (Merck), dimethyl carbonate (DMC, Merck) and tetrahydrofuran (THF, Merck, Germany) were utilized as solvent. Ammonia (25%, Merck) was used to adjust the pH. Hydroxyapatite powder with an average size of 60 nm was supplied by Merck (Germany). Sodium chloride crystals with sizes of 200–400 μm were provided by Merck (Germany) and utilized as porogen.

2.2. In-situ solvothermal process

Four grams of PCL was dissolved into 40 ml acetone under vigorous stirring for 6 h using a magnetic stirrer. The calcium precursor was added into the solution and mixed for 6 h. In a separate beaker, H_3PO_4 was added to acetone and mixed vigorously for 6 h. This solution was added to the PCL solution dropwise to achieve a Ca:P molar ratio of 1.67. The concentration of HA particles in the polymer matrix was set to 20 wt%. The HA concentration was selected based on the results of Rezaei et al. [30] that showed the highest tensile strength could be attained in PCL-20%HA nanocomposites. Ammonia was used to control the pH of the final sol to ~10. This sol was transferred to a sealed autoclave and stirred vigorously for 24 h at different temperatures ranging from 60 to 150 °C. It is pertinent to point out that, some studies have reported that PCL can react with ammonia at temperatures roughly above 200 °C [35,36]; hence, the chemical nature of PCL is not affected in the examined range. The prepared PCL/HA nanocomposite was poured into a Petri dish and dried for 24 h at room temperature.

2.3. Fabrication of porous scaffolds

To prepare PCL/HA scaffolds, the nanocomposite film was dissolved in DMC under vigorous stirring for 8 h using a magnetic stirrer. To create open and large pores, sodium chloride crystals were added to the polymeric solution (30 vol%) and stirred for 2 h. The mixture was then poured into cylindrical aluminium moulds (1 cm diameter and 1.5 cm height) and freeze-dried for 24 h at −70 °C and 0.01 mbar. Afterwards, the scaffolds were immersed in double-distilled water for 7 days to remove the salt and extra ions formed during the solvothermal synthesis. To prepare *ex-situ* PCL/HA nanocomposite, the commercial HA powder and NaCl crystals were added to the polymeric solution and homogenized by stirring for 2 h. Freeze-drying and salt leaching techniques were utilized to prepare highly porous scaffolds (>90% porosity).

2.4. Materials characterization

To analyse the *in-situ* processed HA particles in the polymer matrix, the nanocomposite was dissolved in THF and centrifuged at 3000 rpm for 30 min. The extracted powder was dried and weighted. Morphological analysis was performed on HA and PCL/HA nanocomposites using a MIRA ‖ TESCAN (Czech Republic) and a HITACHI S4160 field-emission scanning electron microscope (FE-SEM, Japan). Phase analysis was conducted using a STOE STADI P X-ray diffractometer (XRD, Germany). Fourier transform infrared (FTIR) spectroscopy (SHIMADZU, Japan) was used to identify the functional groups of HA and to determine the bonds between the ceramic and polymer phases in the composite material. FTIR spectrum was recorded in the range of 500–4000 cm^{-1} with a resolution of 4 cm^{-1}. To determine the hydrophilicity of the prepared films, water contact angle was measured by an OCA15plus video based optical contact angle meter (Dataphysics Instruments GmbH, Filderstadt, Germany). An equal volume of deionized water (4 μl) was placed on the film by means of an electronic syringe unit forming a drop. Photos were taken to record the shape of the drops and the images were analyzed using the instrument software.

2.5. Mechanical examinations

To determine the mechanical properties of the materials and porous scaffolds, tensile and compression tests were utilized on films and cylindrical specimens, respectively. Tensile testing was performed on films with 0.3 mm thickness and a gauge length of 60 mm × 10 mm. Five tensile tests were performed for each film by employing a Hounsfield machine (H10KS, UK) at a cross-head speed of 5 mm/min. For the compression test, cylindrical samples with 15 mm height and 10 mm diameter were examined at a cross-head speed of 1 mm/min. It should be noted that due to the self-lubricating property of the polymer and its highly porous structure, the ratio of diameter to height does not significantly affect the deformation process during upsetting of small samples. The mechanical characteristics of the scaffolds were determined based on the method explained in Ref. [37] for analysing of polymer foams. To evaluate the mechanical properties of the materials without the effect of interconnected pores, dense cylindrical samples of both pristine PCL and PCL/HA nanocomposite (15 mm height and 10 mm diameter) were also prepared by compression moulding at 100 °C/1500 N and examined by the compression test. The average of the mechanical strength with standard deviation was reported. The confidence interval for the average was 90%.

2.6. In vitro bioactivity

In vitro bioactivity of the nanocomposites was evaluated using simulated body fluid (SBF) solution according to the procedure reported in Refs. [38,39]. The composition and pH of the utilized SBF solution are reported in Electronic Supplementary Information (ESI). The scaffolds were soaked in the SBF solution for 7 and 14 days at 37 °C in an incubator. The ratio of the scaffold surface to the volume of SBF solution was 10 mm^2/ml in accordance with Ref. [40]. The formed precipitates on the surface of the scaffolds were examined by FESEM equipped with a energy dispersive X-ray (EDX) spectrometer (VEGA\TESCAN, 15.00 KV). Blue staining of the incubated scaffolds in SBF was performed by a hydrophilic dye utilizing a 0.5% trypan blue solution (w/v) in order to indicate the presence of HA particles on the surface of the scaffolds [19]. After rinsing with absolute ethanol, digital images of the specimens were taken by a digital camera.

2.7. Cell viability

Human osteosarcoma cells (The Pasteur Institute of Iran, Tehran) were utilized for cell viability. It is noteworthy that osteoblast or osteocyte cell line is appropriate to determine the cellular behaviour of the synthesized materials for bone tissue engineering. Since the aim of this study was to show that the materials were not toxic to cells and osteosarcoma cell line was accessible, this cell line was used. The cells were added to a 96-well culture plate at a concentration of 5000 cells/well with 10% fetal bovine serum and 1% antibiotics (100 μg/ml of streptomycin and 100 U/ml of penicillin), and incubated for 24 h. Small specimens (6 mg) were cut from the porous scaffolds and placed in the culture plate after UV sterilizing for 1 h. After 48 and 72 h incubation at 37 °C in a 5% CO_2 atmosphere, the cell viability were evaluated by adding 10 μl of (3-(4,5- Dimethylthiazol-2-yl)-2, 5-diphenyl tetrazolium bromide) (MTT) solution. After 3 h incubation, unreacted dye was removed by aspiration cautiously, and then 150 μl dimethyl sulfoxide was added into each well and shacked for 10 min. The optical density (OD) of the each solution was measured with ELIZA Reader at wavelength of 530 nm and 630 nm. Each assay was repeated 5 times and the average values were reported.

2.8. Statistics

One-way ANOVA ($p < 0.05$, n = 5) was applied using Statistical Package for the Social Sciences (SPSS software, Version 16, IBM, USA) to examine the statistically significant difference between measurements.

3. Results

3.1. Characterization of hydroxyapatite nanorods

A solvothermal process was employed to prepare PCL-based nanocomposites reinforced with HA particles. Fig. 1 shows FE-SEM images of the bioceramic nanoparticles obtained at different processing temperatures. At 60 °C, the particles with irregular shapes are formed. The solvothermal treatment of the polymer/HA precursors at 70 °C yields rod-shape particles with a diameter of ~30 nm and a length of ~230 nm. Processing at higher temperatures forms nanorods with higher diameters (width) and aspect ratios (height to width). At 120 °C, rods with a diameter of about 70 nm with an aspect ratio of 7 are attained. The one-dimensional growth of ceramic nanorods is commonly ascribed to the surface energy of crystal planes as the absorption of cations and anions from the solution varies with the plane surface energy [41,42]. In order to determine the composition of the precipitates, EDS and XRD were employed (Fig. 2). EDS analysis determines that the Ca/P ratio is in the range of 1.6–1.7 (Table 1). It is also noticeable that the chemical composition of the precipitates becomes closer to the stoichiometric Ca/P ratio of HA (1.67 [30]) as the processing temperature is increased. The XRD pattern of the rods prepared at 80 °C is well matched with the standard (JCPDS 09–432) and commercial (Merck) HA particles, although residual amounts of PCL is also detectable after the separation process (at $2\theta = 15.7°$, 21.5° and 23.8°). The characteristic peaks of HA are relatively broad that is induced by their small (crystallite) sizes and their semi-crystalline nature [43]. According to the peak intensity ratio (I_{112}/I_{300}) [44], the crystallinity of the particles is estimated to be 20%. The relatively low processing temperature yields poorly crystalline HA particles, which favours bone regeneration *in vivo* [30,45]. It is noteworthy that bone regeneration could be weak in highly crystalline porous HA ceramics [46]. Moreover, no characteristic peaks of calcium carbonates are visible both in XRD analysis (with considering the detection limit of XRD) and FTIR examination (see next section). This observation reveals one of the advantages of the *in-situ* solvothermal process compared to the most wet-chemical derived hydroxyapatite especially sol–gel routs [30].

3.2. Polymer matrix nanocomposites

The FTIR spectrum of the PCL/nanorod-HA nanocomposite prepared at 80 °C is shown in 3a. Most corresponding bands of HA and PCL materials are visible in the spectrum that confirms the formation of both compounds in the nanocomposite. The C=O, C–O, and C=H bands are related to PCL. The first indication of the hydroxyapatite formation is the form of broad FTIR band cantered at about 1000–1100 cm^{-1} [47]. The bands at 960–965 cm^{-1} and 565–600 cm^{-1} correspond to n_1 and n_4 symmetric P–O stretching vibration of the $PO3^{-4}$ ion [48,49]. Moreover, the peaks at 1420 and 1460 cm^{-1} are related to OH^- bonds in HA [28]. As compared to pristine HA and PCL, small peak shift could indicate formation of bonds between HA and PCL during the chemical process [30]. Fig. 3b and c shows SEM micrographs of the prepared scaffolds by the salt leaching method. The SEM images indicate that the scaffold has a porous structure with pore sizes in the range of 10–200 μm. The effect of HA particles on the hydrophilicity of PCL films is

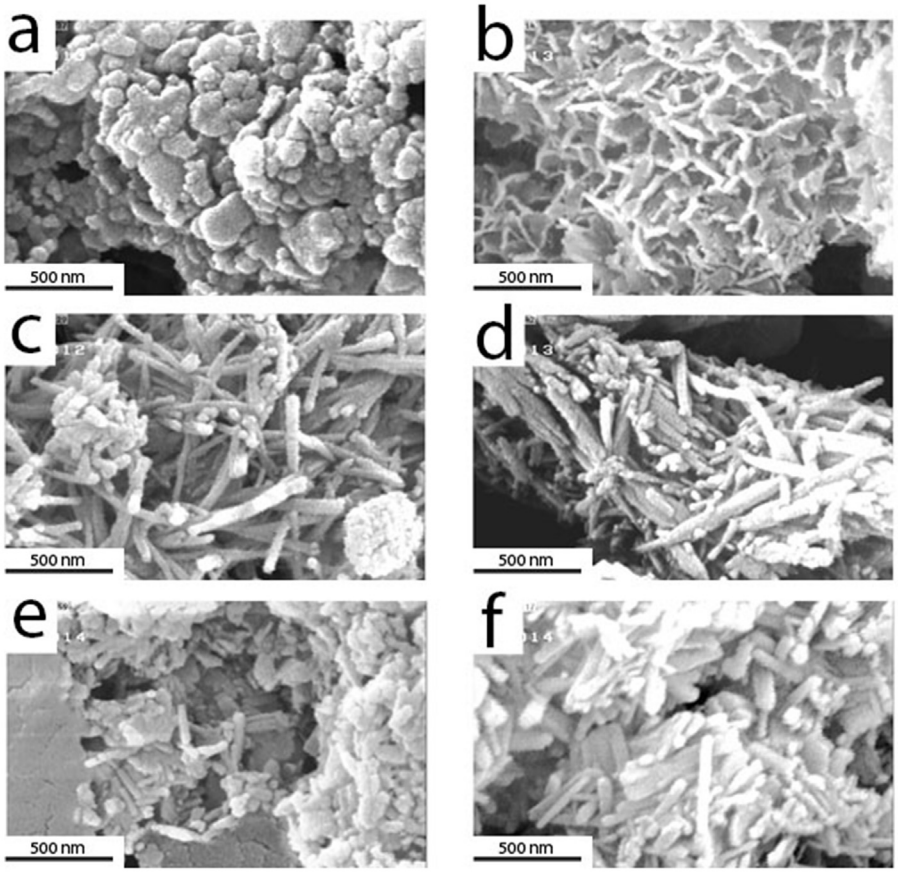

Fig. 1. FE-SEM micrographs of HA powder prepared by *in-situ* solvothermal process at different temperatures (°C) of a) 60, b) 70, c) 80, d) 90, e) 120, and f) 150.

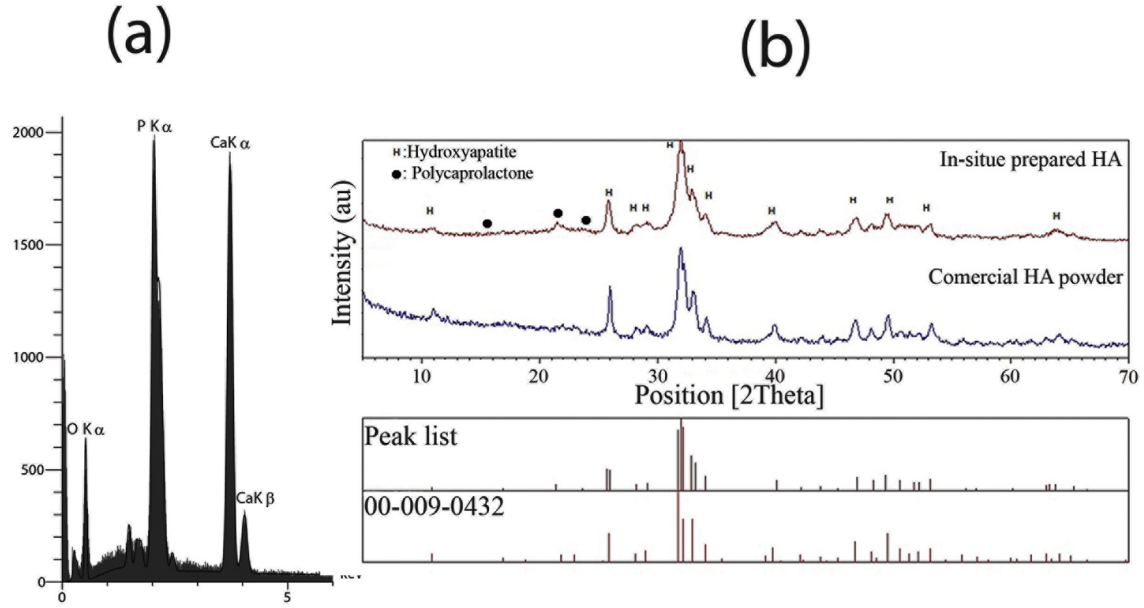

Fig. 2. EDS spectrum and XRD pattern of HA particles *in-situ* synthesized by solvothermal processing at 80 °C. The XRD pattern of commercial HA powder (Merck) is included for comparison.

shown in Fig. 3d. As expected, HA particles reduce the hydrophobicity of PCL matrix. The difference between the *in-situ* and *ex-situ* particles is not conspicuous, though the surface roughness and surface distribution of the particles could influence the contact angle.

Table 1
Effect of processing temperature on the Ca/P ratio of the in-situ synthesized particles as determined by EDS.

Temperature (°C)	60	70	80	90
Ca/P atomic ratio	1.60	1.65	1.66	1.70

3.3. Mechanical property

Fig. 4a shows compressive stress-strain curves for the PCL and *in-situ* PCL/HA(20 wt%) nanocomposite prepared by compression moulding (without porosity). The curves are the average of five examinations. The elastic modulus and strength of the materials were determined by the procedure explained in Ref. [37]. The results are reported in Table 2. As seen, the presence of HA nanorods increases the elastic modulus and strength by ca. 50% and 26%, respectively. Fig. 4b shows the compression curves for highly porous scaffolds (>90%) prepared by freeze-drying and salt leaching processes (averaged over 5 samples). Under compression load, all curves display the typical characteristics of porous polymeric foams, in which a linear elastic region appears at low strain followed by a long plateau region and finally a rapid increasing region due to the material densification [13]. The effect of HA particles on the mechanical strength is less pronounced than that of dense specimens due to the role of open pores on the flow behaviour of the polymer matrix under loading. Meanwhile, the *in-situ* processed nanocomposite yields improved mechanical performance as compared to the *ex-situ* one. This enhancement can be attributed to the morphological effect (nanorod versus spherical particles), interfacial bonding between HA and PCL, and possibly better distribution of the nanoparticles in the polymer matrix during *in-situ* processing [30–32]. Similar results are obtained under tensile loading for films (Fig. 4c). The strength of the nanocomposite prepared by the *in-situ* method is about 15% higher than the ex-situ one (Table 2). Although the addition of HA nanoparticles is accompanied with reduction of ductility, the detrimental effect of the *in-situ* processed bioceramics is less than the *ex-situ* nanocomposite.

3.4. Bioactivity

After immersion of PCL/HA(20%) scaffold in SBF for 14 days, SEM and EDAX analyses were conducted. Fig. 5a shows that calcium phosphate crystals cover the surface of the scaffold. The

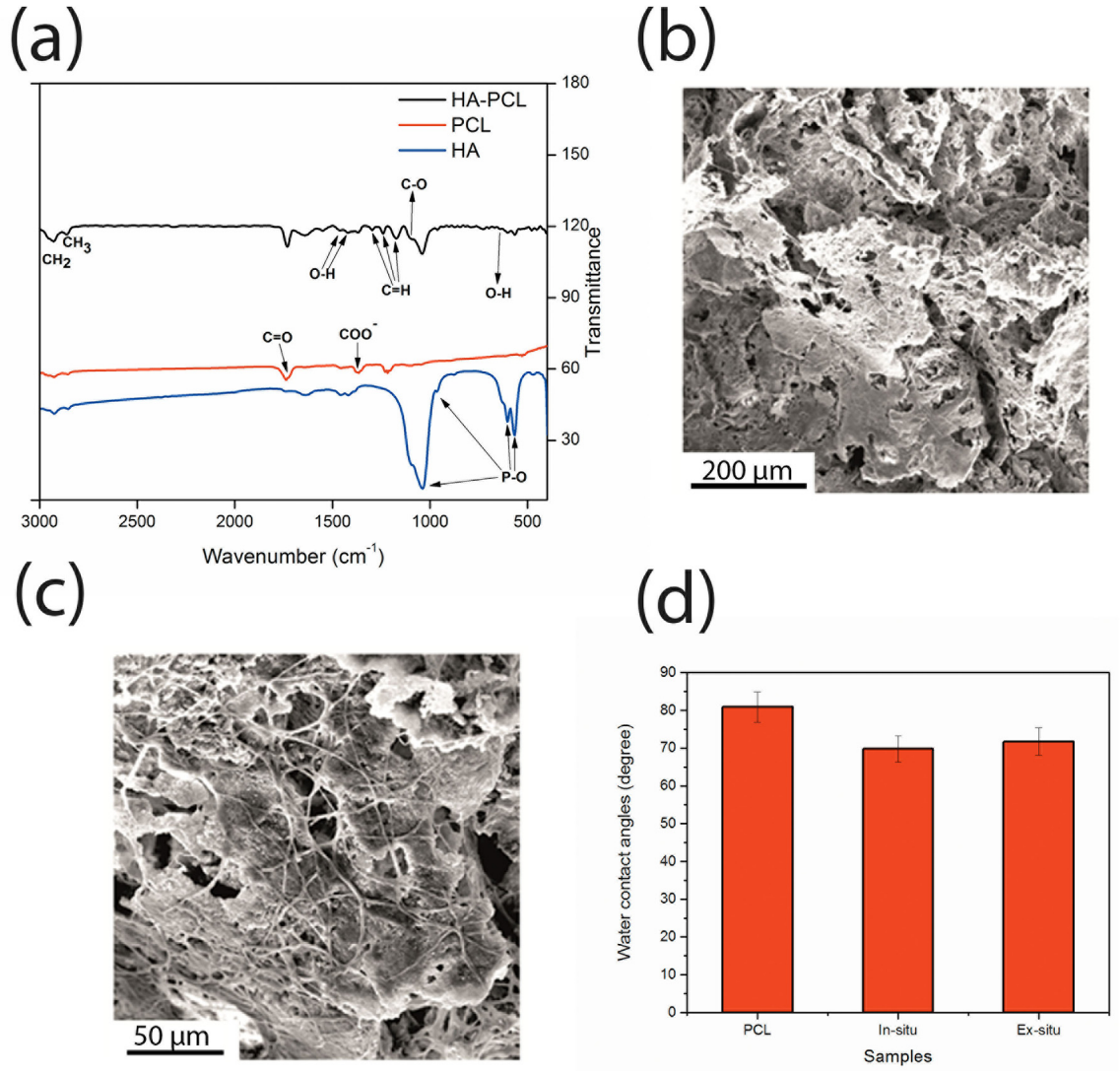

Fig. 3. Characterization of PCL/nanorod-HA nanocomposite prepared by *in-situ* solvothermal processing at 80 °C. (a) FTIR spectrum as compared to pristine HA and PCL. (b,c) SEM images of PCL/HA scaffolds prepared by the salt leaching method at two different magnifications. (d) Effect of HA nanoparticles on the hydrophilicity of PCL films prepared by solvent casting methods.

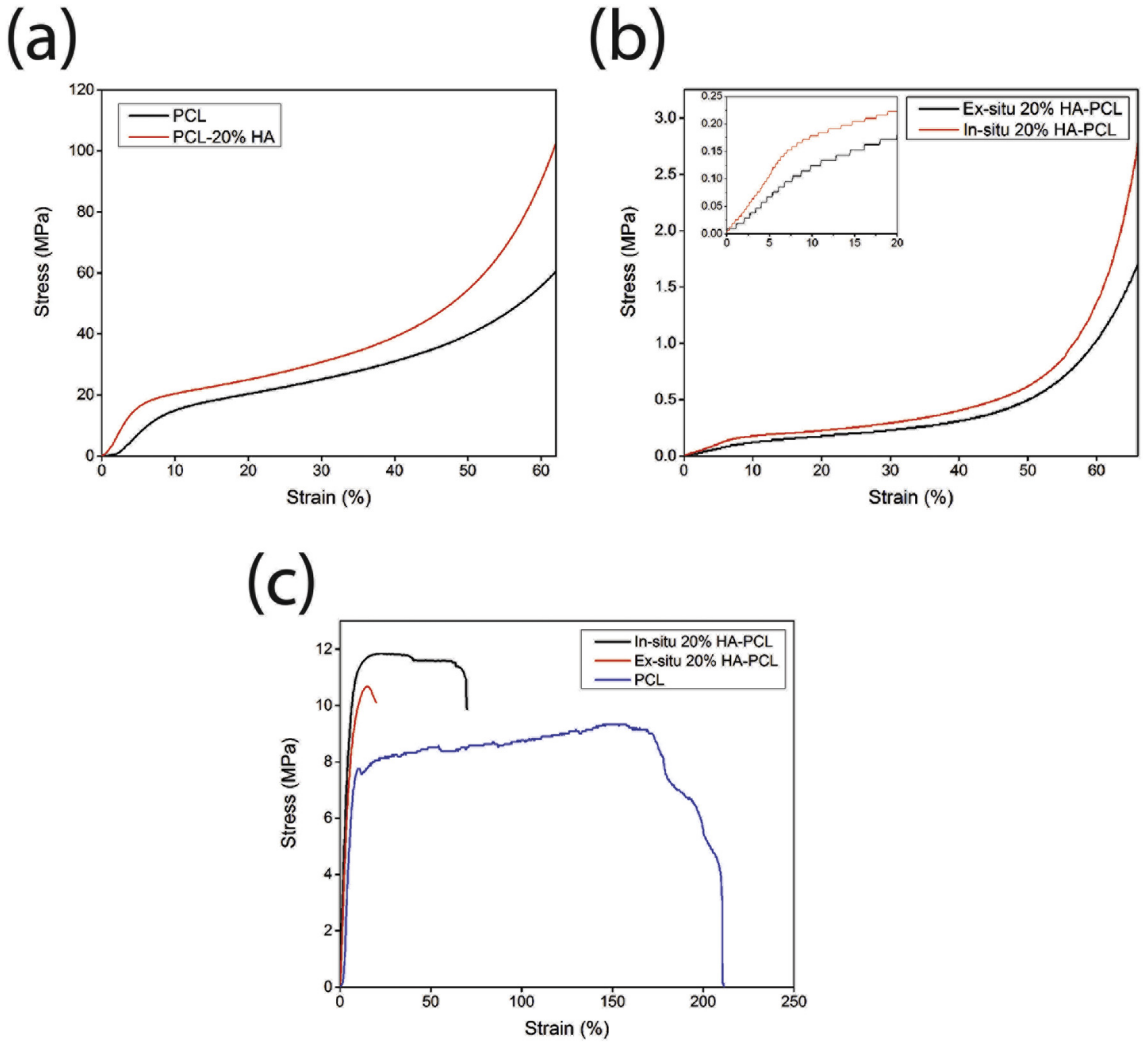

Fig. 4. Engineering stress-strain curves for PCL and PCL/HA(20%) nanocomposites. (a) Compression curves of dense PCL and *in-situ* PCL/HA specimens prepared by compression moulding. (b) Compression curves for PCL/HA porous scaffolds. (c) Tensile behaviour of PCL and PCL/HA nanocomposite films.

Table 2
Mechanical properties of PCL and PCL-20%HA nanocomposites.

Property (MPa)	Test	Sample	PCL	*Ex-situ* nanocomposite	*In-situ* nanocomposite
Elastic modulus	Compression	Dense cylinder	160.8 ± 7	–	241.6 ± 12
	Compression	Porous scaffold	–	1.39 ± 0.048	1.99 ± 0.076
	Tensile	Film	106 ± 6	117 ± 3	126 ± 4
Strength	Compression	Dense cylinder	15 ± 0.2	–	19 ± 0.4
	Compression (in kPa)	Porous scaffold	–	114 ± 11	159 ± 7
	Tensile	Film	9.3 ± 0.3	10.7 ± 0.2	11.8 ± 0.2

– Not measured.

precipitates are also formed on the internal pore walls of the scaffold as a result of the high concentration of SBF which induces a fast and uniform deposition of hydroxyapatite on the nanocomposite scaffolds. The Ca/P ratio of the precipitates is approximately 1.67, revealing the formation of HA particles upon immersion in SBF. Fig. 5b shows digital images of the nanocomposite scaffold treated by the trypan blue solution (0.5 w/v%). The blue colour of the specimens indicates the presence of HA particles on the surface of the scaffolds. It is noted that the blue colour is intensified by immersion in SBF, particularly at prolonged times.

3.5. Cytotoxicity

Cell viability of PCL/HA(20%) nanocomposites was studied in human osteosarcoma cell lines by MTT assay (Fig. 6). The composite scaffolds exhibit higher cell viability than that of the control with an improvement in the viability with the incubation time. Since the increase in the viability is a direct measure of living cells [29], the results suggest that cell proliferation has taken place. The higher cell viability of the *in-situ* prepared PCL/HA scaffold compared to the *ex-situ* scaffold can be attributed to the morphology and crystallinity of the HA crystals [14,46].

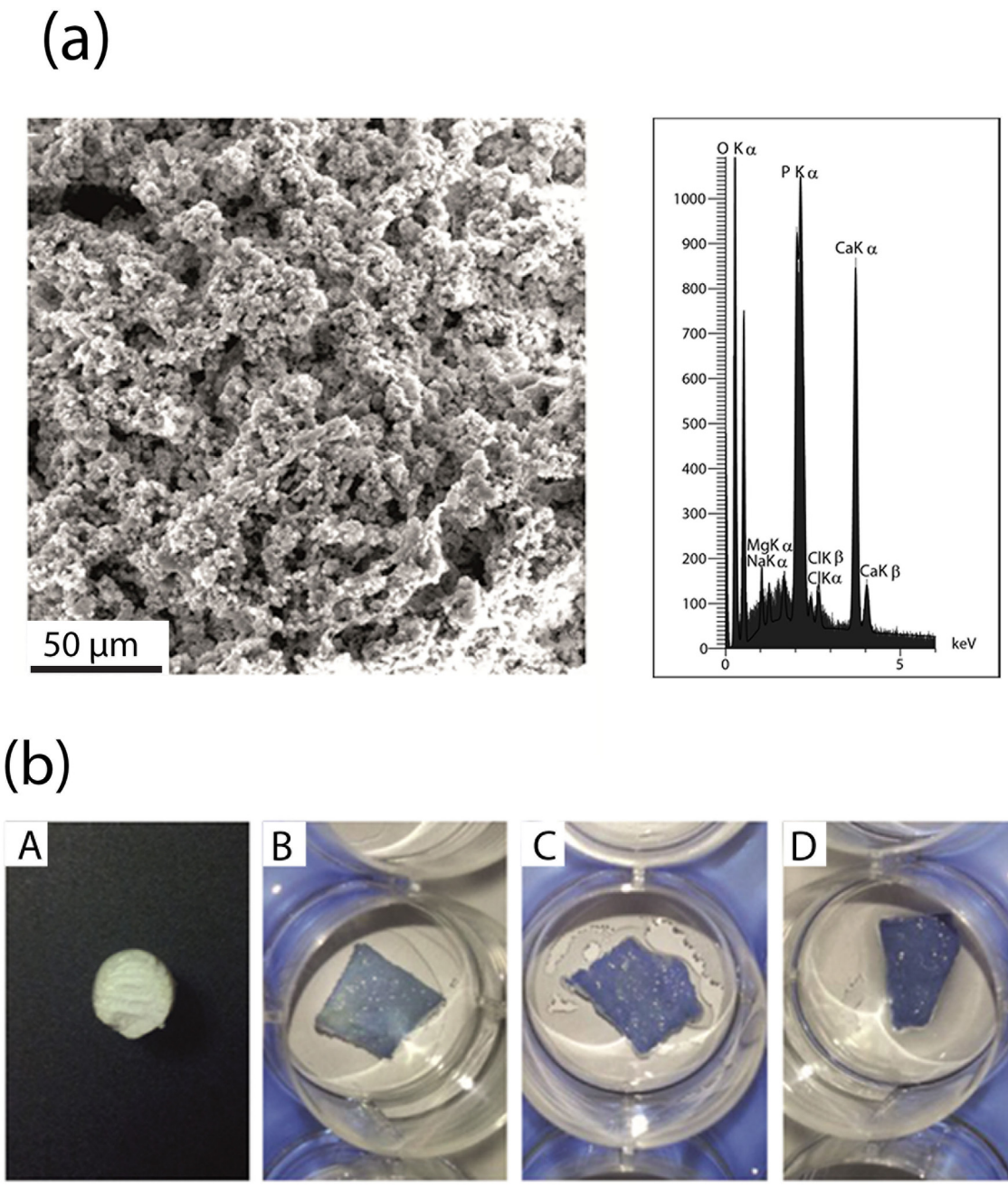

Fig. 5. (a) SEM images and EDS spectrum of the *in-situ* synthesized PCL/HA nanocomposite after 14 days immersion in SBF. (b) Digital images of PCL/HA nanocomposite (A) before and (B–D) after trypan blue treatment: The scaffolds (B) was treated before immersing in SBF while the others were after (C) 7 days and (D) 14 days immersion.

4. Discussion

In this work, HA nanorods were synthesized in alkaline conditions in the presence of PCL through solvothermal methods. The mechanism of the crystal formation is schematically shown in Fig. 7a. The process includes two steps of nucleation and growth. In the initial stages, nucleuses of HA are formed in the supersaturated medium of Ca and P ions [50]. Afterwards, the nucleuses are grown in the high-pressure vessel. It is demonstrated that temperature and pH are the most significant factors affecting the structural and morphological characteristics of HA nanoparticles [51]. The atomic structure of the HA unit cell makes the interfacial free energy of the (001) plane (perpendicular to the c-axis) greater than the other faces [52]. Therefore, at a high critical concentration of ions in the bulk solution, directional growth occurs as the ions migrate to the (001) face, causing the crystals to grow exclusively along the c-axis of HA [53]. Increasing of the processing temperature affects the kinetics of nucleation and growth. The effect of temperature on the size and aspect ratio of the prepared HA particles are shown in Fig. 7b. At higher temperatures, the number of nucleuses is increased and at the same time the growth rate is enhanced due to the faster diffusion rate [51]. The higher temperature also facilitates the crystal growth as the role of surface tension on specific crystal facets is reduced. As a result, both width and length of the crystals increase with increasing the temperature. Nevertheless, at high temperatures there is a counterbalance between rapid diffusion

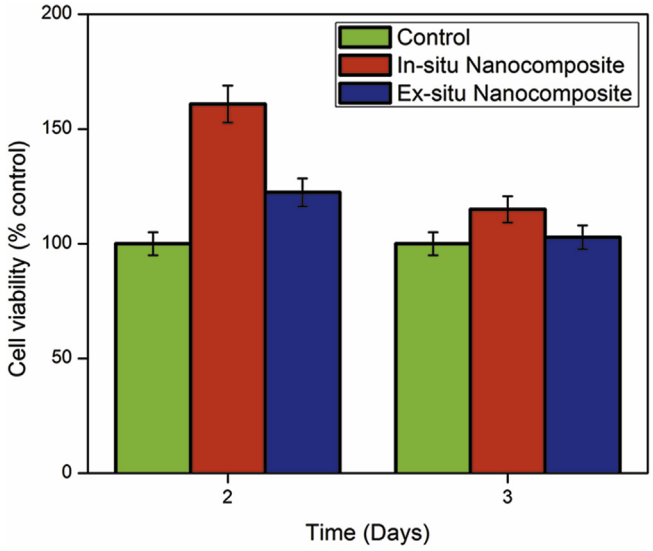

Fig. 6. Cell viability of PCL/HA(20%) nanocomposites incubated in human osteosarcoma cell lines. The statistically significant difference was determined by ANOVA, $P < 0.05$, $n = 5$.

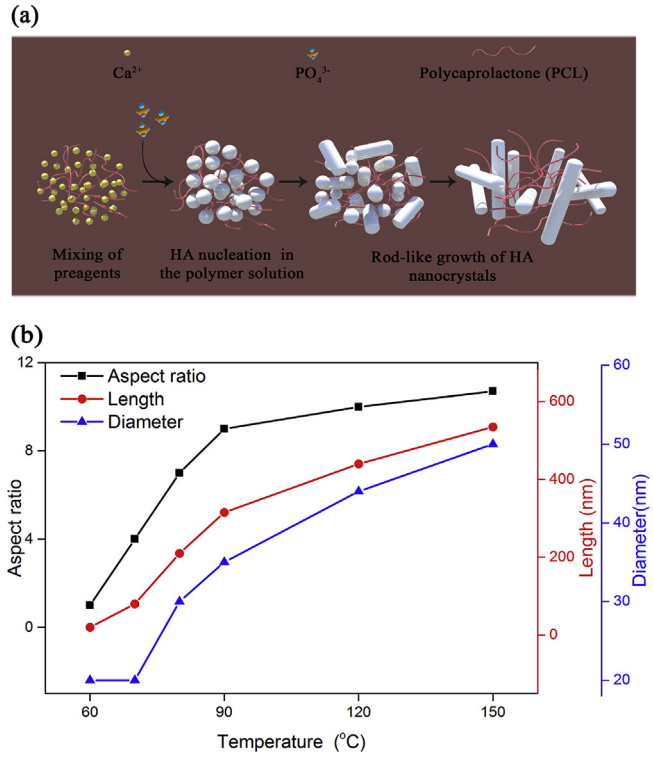

Fig. 7. (a) Schematic presentation of nucleation and growth of HA particles in the polymer matrix (PCL) during solvothermal processing in an alkaline solution (pH = 10). (b) Effect of temperature on the dimensions of *in-situ* synthesized HA particles.

rate of ions and their saturation concentration in the solution [52]. In fact, high number of nucleuses along with their rapid growth decreases the ion concentration into a level where the overall chemical potential of the bulk solution decreases. This makes it difficult for the diffusion flux of ions to preferentially go to the (001) face of HA. It was also demonstrated that the prepared nanoparticles are stoichiometric HA with a low degree of crystallinity (Fig. 2). Previous studies have shown that crystalline HA particles are commonly synthesized at temperatures >120 °C [51], at which the driving forces to order atoms and move them to the crystalline sites are provided. It is thus suggestible that at relatively low processing temperature (80 °C), HA particles with a low crystallinity are formed due to low driving force for the diffusion of atoms.

The mechanical properties of nanocomposites are influenced by the uniform dispersion of filler into the matrix and good interfacial bonding between them [1,2]. We employed *in-situ* solvothermal processing to attain a more uniform dispersion of HA nanorods in the PCL matrix, and possibly improved chemical bonding. Nevertheless, FTIR spectroscopy showed no strong chemical bonding between HA and PCL. On the other hand, we measured an improved mechanical strength for the *in-situ* processed composite compared with the *ex-situ* one. Therefore, we concluded that the improved strength could mainly be attributed to better distribution of the filler in the polymer matrix. It was also observed that this effect was less influenced for the porous scaffolds prepared by freeze drying and salt leaching methods. This is because of high porosity content of the scaffolds (>90%), which significantly affects the mechanical strength of the nanocomposites.

In vitro bioactivity assay also showed that the *in-situ* processed nanocomposite has higher activity in SBF than the *ex-situ* one. It is known that HA particles act as heterogeneous nucleation sites for the subsequent deposition of crystals from the solution whit a kinetics dependency on the morphology, surface area and crystallography preference of the HA particles [14]. Since HA nanorods with low crystallinity were synthesized, higher bioactivity compared with the regular-shaped particles and highly crystalline HA particles was attained. The low crystallinity of the HA nanorods, which are thermodynamically less stable, provided higher dissolubility in the solution induced by solution-mediated dissolution (rather than cellular/enzyme action) [54–56]. In other words, the dissolved ions facilitated nucleation and growth of subsequent natural/biological HA. On the other hand, cell viability assay showed that the prepared scaffolds are not cytotoxic. Both composites exhibited better response to the cells compared to the control one. Probably the HA particles provided a surface suitable for cell attachment and proliferation [57] along with the presence of large pores (100–200 μm) which promote proliferation of cells [30]. A higher cell proliferation on the *in-situ* rod-like HA-PCL nanocomposite compared to the ex-situ one can be attributed to the effect of HA morphology and its low crystallinity [58]. Blackwood and Seah [59] have reported that HA nanorods have a better influence on the cell proliferation and bioactivity. On the other hand, Xu et al. [60] also have shown that spherical nanoparticles (mean diameter of 20 nm) induced higher expressions of metabolic enzymes, which suggest that spherical nanoparticles might be more potentially hazardous to the osteoblasts as compared to the nanorods.

5. Conclusions

A solvothermal process was employed to prepare nanorod HA(20%)-reinforced PCL composite scaffolds. It was shown that the aspect ratio of the HA nanorods was increased from 2 to 10 by increasing the processing temperature from 70 to 150 °C. Processing at 80 °C was found to be suitable to attain low crystalline HA nanorods with an aspect ratio of about 4 without severe agglomeration in the PCL matrix. The prepared nanocomposite exhibited better bioactivity in SBF than the ex-situ prepared PCL/HA nanocomposite through mixing of the constituents. The mechanical strength was also higher. The *in vitro* cellular assays suggested the scaffolds of nanorod-HA/PCL and HA/PCL were nontoxic to human osteosarcoma cell. Therefore, the prepared scaffolds

could be promising for non-load bearing bone regeneration because of their good mechanical properties and ability to promote apatite growth.

Acknowledgments

The authors wish to thank Dr. N. Lotfibakhshaiesh (School of Advanced Technologies in Medicine, Tehran University of Medical Sciences, Tehran, Iran) for conducting the cellular tests. AS wish to thank funding support from Sharif University of Technology (SUT, No. G930305) and Iran National Science Foundation (INSF No. 95-S-48740).

Appendix A. Supplementary data

Supplementary data related to this article can be found at http://dx.doi.org/10.1016/j.bioactmat.2017.04.004.

References

[1] J.M. Karp, P.D. Dalton, M.S. Shoichet, Scaffolds for tissue engineering, MRS Bull. Cell Solids 28 (2003) 301–306.
[2] J.R. Porter, T.T. Ruckh, K.C. Popat, Bone tissue engineering: a review in bone biomimetics and drug delivery strategies, Biotechnol. Prog. 25 (2009) 1539–1560.
[3] S. Weiner, H.D. Wagner, The material bone: structure-mechanical function relations, Annu. Rev. Mater. Sci. 28 (1998) 271–298.
[4] C. Hellmich, F.J. Ulm, Average hydroxyapatite concentration is uniform in extracollagenousultrastructure of mineralized tissue, Biomech. Model. Mechanobiol. 2 (2003) 21–36.
[5] L.L. Hench, D.L. Wheeler, D.C. Greenspan, Molecular control of bioactivity in sol-gel glasses, J. Sol Gel Sci. Technol. 13 (1998) 245–250.
[6] Y. Liu, G. Wang, Y. Cai, H. Ji, G. Zhou, X. Zhao, et al., In vitro effects of nano-phase hydroxyapatite particles on proliferation and osteogenic differentiation of bone marrow-derived mesenchymal stem cells, J. Biomed. Mater Res. 90 (2009) 1083–1091.
[7] D.W. Hutmacher, J.T. Schantz, C.X.F. Lam, K.C. Tan, T.C. Lim, State of the art and future directions of scaffold-based bone engineering from a biomaterials perspective, J. Tissue Eng. Regen. Med. 1 (2007) 245–260.
[8] H.L. Nichols, N. Zhang, J. Zhang, D. Shi, S. Bhaduri, X. Wen, Coating nano-thickness degradable films on nanocrystalline hydroxyapatite particles to improve the bonding strength between nanohydroxyapatite and degradable polymer matrix, J. Biomed. Mater Res. 82A (2007) 373–382.
[9] H. Zhou, J. Lee, Nanoscale hydroxyapatite particles for bone tissue engineering, Acta Biomater. 7 (2011) 2769–2781.
[10] M.G. Raucci, V. D'Antò, V. Guarino, E. Sardella, S. Zeppetelli, P. Favia, et al., Biomineralized porous composite scaffolds prepared by chemical synthesis for bone tissue regeneration, Acta Biomater. 6 (2010) 4090–4099.
[11] P. Fabbri, F. Bondioli, M. Messori, C. Bartoli, D. Dinucci, F. Chiellini, Porous scaffolds of polycaprolactone reinforced with in situ generated hydroxyapatite for bone tissue engineering, J. Mater Sci. Mater. Med. 21 (2010) 343–351.
[12] M.G. Raucci, V. Guarino, L. Ambrosio, Hybrid composite scaffolds prepared by sol–gel method for bone regeneration, Compos Sci. Technol. 70 (2010) 1861–1868.
[13] Y. Wang, L. Liu, S. Guo, Characterization of biodegradable and cytocompatible nano-hydroxyapatite/polycaprolactone porous scaffolds in degradation in vitro, Polym. Degrad. Stab. 95 (2010) 207–213.
[14] S.K. Padmanabhan, A. Balakrishnan, M.C. Chu, Y.J. Lee, T.N. Kim, S.J. Cho, Sol–gel synthesis and characterization of hydroxyapatite nanorods, Particuology 7 (2009) 466–470.
[15] D.O. Costa, S.J. Dixon, A.S. Rizkalla, One- and three-dimensional growth of hydroxyapatite nanowires during Sol–Gel–Hydrothermal synthesis, ACS Appl. Mater. Interfaces 4 (2012) 1490–1499.
[16] A. Joseph Nathanael, D. Mangalaraj, P. Chi Chen, N. Ponpandian, Enhanced mechanical strength of hydroxyapatite nanorods reinforced with polyethylene, J. Nanopart. Res. 5 (2011) 1841–1853.
[17] H. Zhou, J. Lee, Nanoscale hydroxyapatite particles for bone tissue engineering, Acta Biomater. 7 (2011) 2769–2781.
[18] E. Aydin, J.A. Planell, V. Hasirci, Hydroxyapatite nanorod-reinforced biodegradable poly(l-lactic acid) composites for bone plate applications, J. Mater. Sci. Mater. Med. 22 (2011) 2413–2427.
[19] J.J. Mao, X. Xin, M. Hussain, Continuing differentiation of human mesenchymal stem cells and induced chondrogenic and osteogenic lineages in electrospun PLGA nanofiber scaffold, Biomaterials 28 (2007) 316–325.
[20] A.P.D. Elfick, Poly(ε-caprolactone) as a potential material for a temporary joint spacer, Biomaterials 23 (2002) 4463–4467.
[21] L. Shor, S. Cuceri, X. Wen, M. Gandhi, W. Sun, Fabrication of three-dimensional polycaprolactone/hydroxyapatite tissue scaffolds and osteoblast-scaffold interactions in vitro, Biomaterials 28 (2007) 5291–5297.
[22] S.C. Baker, G. Rohman, J. Southgate, N.R. Cameron, The relationship between the mechanical properties and cell behaviour on PLGA and PCL scaffolds for bladder tissue engineering, Biomaterials 30 (2009) 1321–1328.
[23] C.M. Agrawal, R.B. Ray, Biodegradable polymeric scaffolds for musculoskeletal tissue engineering, J. Biomed. Mater. Res. 55 (2001) 141–150.
[24] V. Guarino, F. Causa, P.A. Netti, G. Ciapetti, S. Pagani, D. Martini, et al., The role of hydroxyapatite as solid signal on performance of PCL porous scaffolds for bone tissue regeneration, J. Biomed. Mater Res. B 86B (2008) 548–557.
[25] S.J. Heo, S.E. Kim, Y.T. Hyun, D.H. Kim, H.M. Lee, Y.M. Hwang, et al., In vitro evaluation of poly ε-caprolactone/hydroxyapatite composite as scaffolds for bone tissue engineering with human bone marrow stromal cell, Key Eng. Mater 342–343 (2007) 369–372.
[26] E. Tamjid, R. Bagheri, M. Vossoughi, A. Simchi, Effect of particle size on the in vitro bioactivity, hydrophilicity and mechanical properties of bioactive glass-reinforced PCL composites, J. Mater. Sci. Eng. C 31 (2011) 1526–1533.
[27] E. Tamjid, R. Bagheri, M. Vossoughi, A. Simchi, Effect of TiO2 morphology on the in vitro bioactivity and mechanical properties of polycaprolactone/TiO2 nanocomposites for tissue engineering, Mater. Lett. 65 (2011) 2530–2533.
[28] J.P. Chen, Y.S. Chang, Preparation and characterization of composite nanofibers of polycaprolactone and nanohydroxyapatite for osteogenic differentiation of mesenchymal stem cells, Colloids Surf. B Biointerfaces 86 (2011) 169–175.
[29] L. Li, G. Li, J. Jiang, X. Liu, L. Luo, K. Nan, Electrospun fibrous scaffold of hydroxyapatite/poly (e-caprolactone) for bone regeneration, J. Mater. Sci. Mater. Med. 23 (2012) 547–554.
[30] A. Rezaei, M.R. Mohammadi, In vitro study of hydroxyapatite/polycaprolactone nanocomposite synthesized by an in situ sol–gel process, Mater. Sci. Eng. C 33 (2013) 390–396.
[31] M.G. Raucci, V. Guarino, L. Ambrosio, Hybrid composite scaffolds prepared by sol–gel method for bone regeneration, Compos. Sci. Technol. 70 (2010) 1861–1868.
[32] W.Y. Choi, H.E. Kim, S.Y. Oh, Y.H. Koh, Synthesis of poly(ε-caprolactone)/hydroxyapatite nanocomposites using in-situ co-precipitation, Mater. Sci. Eng. C 30 (2010) 777–780.
[33] X. Zheng, S. Zhou, Y. Xiao, X. Yu, B. Feng, In situ preparation and characterization of a novel gelatin/poly(D,L-lactide)/hydroxyapatite nanocomposite, J. Biomed. Mater. Res. Part B Appl. Biomater. 91B (2009) 181–190.
[34] T. Goto, I.Y. Kim, K. Kikuta, C. Ohtsuki, Hydrothermal synthesis of composites of well-crystallized hydroxyapatite and poly(vinyl alcohol) hydrogel, Mater. Sci. Eng. C 32 (2012) 397–440.
[35] Y. Honda, Z. Osawa, Microbial denitrification of wastewater using biodegradable polycaprolactone, Polym. Degrad. Stab. 76 (2002) 321–327.
[36] Muneeswaran M, Giridharan N, Velmathi S. Solvent-free ring opening polymerization of ε-caprolactone and electrical properties of polycaprolactone blended $BiFeO_3$ nanocomposites. RSC Adv.; (on published).
[37] Y.F. Chou, W.A. Chiou, Y. Xu, J.C.Y. Dunn, B.M. Wu, The effect of pH on the structural evolution of accelerated biomimetic apatite, Biomaterials 25 (2004) 5323–5331.
[38] T. Kokubo, H.-M. Kim, M. Kawashita, Novel bioactive materials with different mechanical properties, Biomaterials 24 (2003) 2161–2175.
[39] D.V.W.M. De Vries, Characterization of Polymeric Foams, MSc Thesis, Eindhoven University of Technology, 2009.
[40] M. Tanahashi, K. Hata, T. Kokubo, M. Minoda, T. Miyamoto, T. Nakamura, et al., in: T. Yamamuro, T. Kokubo, T. Nakamuro (Eds.), Bioceramics, Kobunshi Kankokai, Kyoto, 1992, pp. 57–64.
[41] V. Guarino, P. Taddei, M. Di Foggia, C. Fagnano, G. Ciapetti, L. Ambrosio, The influence of hydroxyapatite particles on in vitro degradation behavior of poly e-caprolactone–based composite scaffolds, Tissue Eng. Part A 15 (2009) 3655–3668.
[42] W.J. Li, E.W. Shi, W.Z. Zhong, Z.W. Yin, Growth mechanism and growth habit of oxide crystals, J. Cryst. Growth 203 (1999) 186–196.
[43] L.A. Azaroff, Elements of of X-Ray Crystalography, Mcagraw-Hill, New York, 1968, pp. 38–42.
[44] Y.X. Pang, X. Bao, Influence of temperature, ripening time and calecinations on the morphology and crystallinity of hydroxyapatite nanopowders, J. Eur. Ceram. Soc. 23 (2003) 1697–1704.
[45] E.M. Wouterson, F.Y.C. Boey, X. Hu, S.C. Wong, Specific properties and fracture toughness of syntactic foam: effect of foam microstructures, Compos. Sci. Technol. 65 (2005) 1840–1850.
[46] J. Dong, T. Uemura, H. Kojima, M. Kikuchi, J. Tanaka, T. Tateishi, Application of low-pressure system to sustain in vivo bone formation in osteoblast/porous hydroxyapatite composite, Mater Sci. Eng. C 17 (2001) 37–43.
[47] H.K. Varma, S.S. Babu, Synthesis of calcium phosphate bioceramics by citrate gel pyrolysis method, Ceram. Int. 31 (2005) 109–114.
[48] M. Kawata, H. Uchida, K. Itatani, I. Okada, S. Koda, M. Aizawa, Development of porous ceramics with well-controlled porosities and pore size from apatite fibers and their evaluations, J. Mater. Sci. Mater. Med. 15 (2004) 817–823.
[49] F. Miyaji, Y. Kono, Y. Suyama, Formation and structure of zink-substituted calcium hydroxyapatite, Mater. Res. Bull. 40 (2005) 209–213.
[50] J.D. Chen, Y.J. Wang, K. Wei, S.H. Zhang, X.T. Shi, Self-organization of hydroxyapatite nanorods through oriented attachment, Biomaterials 28 (2007) 2275–2280.
[51] M. Sadat-Shojai, M.-T. Khorasani, E. Dinpanah-Khoshdargi, A. Jamshidi, Synthesis methods for nanosized hydroxyapatite with diverse structures, Acta Biomater. 9 (2013) 7591–7621.

[52] T.G. Kim, B. Park, Synthesis and growth mechanisms of one-dimensional strontiumhydroxyapatite nanostructures, Inorg. Chem. 44 (2005) 9895–9901.
[53] X.G. Peng, Z.A. Peng, Mechanisms of the shape evolution of CdSe nanocrystals, J. Am. Chem. Soc. 123 (2001) 1389–1395.
[54] H. Oonishi, L.L. Hench, J. Wilson, F. Sugihara, E. Tsuji, M. Matsuura, Quantitative comparison of bone growth behavior in granules of Bioglass, glass-ceramic, and hydroxyapatite, J. Biomed. Mater Res. 51 (2000) 37–46.
[55] H. Oonishi, S. Kushitani, E. Yasukawa, H. Iwaki, L.L. Hench, J. Wilson, et al., Particulate bioglass compared with hydroxyapatite as a bone graft substitute, Clin. Orthop. Relat. Res. (1997) 316–325.
[56] D.L. Wheeler, E.J. Eschbach, R.G. Hoellrich, M.J. Montfort, D.L. Chamberland, Assessment of resorbable bioactive material for grafting of critical-size cancellous defects, J. Orthop. Res. 18 (2000) 140–148.
[57] M. Vogel, C. Voigt, C. Knabe, R.J. Radlanski, U.M. Gross, C.M. Muller-Mai, Development of multinuclear giant cells during the degradation of Bioglass_ particles in rabbits, J. Biomed. Mater Res. Part A 70 (2004) 370–379.
[58] Y. Cai, Y. Liu, W. Yan, Q. Hu, J. Tao, M. Zhang, Role of hydroxyapatite nanoparticle size in bone cell proliferation, J. Mater Chem. 17 (2007) 3780–3787.
[59] D. Blackwood, K. Seah, Electrochemical cathodic deposition of hydroxyapatite: improvements in adhesion and crystallinity, Mater Sci. Eng. C 29 (2009) 1233–1238.
[60] J.L. Xu, K.A. Khor, J.J. Sui, J.H. Zhang, W.N. Chen, Protein expression profiles in osteoblasts in response to differentially shaped hydroxyapatite nanoparticles, Biomaterials 30 (2009) 5385–5391.